CHEMISTRY JOURNAL OF MOLDOVA. General, Industrial and Ecological Chemistry. 2025, 20(1), 79-85
ISSN (p) 1857-1727 ISSN (e) 2345-1688
http://cjm.ichem.md
https://doi.org/10.19261/cjm.2025.1279

HYDROGEN STORAGE PERFORMANCE OF ACTIVATED NATURAL ZEOLITE AND ITS MODIFICATION WITH ACTIVATED CHARCOAL

Latifah Hauli [a*], Chika Lutfi Adiningrum [b], Muhammad Safaat [a], Indri Badria Adilina [a], Silvester Tursiloadi [a], Lenny Marlinda [b], Dian Susanthy [c], Muflikhah Muflikhah [d]

[a]*Research Center for Chemistry, National Research and Innovation Agency (BRIN), B.J. Habibie Science and Technology Area, 60, Raya Puspiptek str., Setu, South Tangerang, Banten 15314, Indonesia*
[b]*Department of Chemistry, Faculty of Science and Technology, Universitas Jambi, 15, Jambi-Muara Bulian No.KM. str., Jambi Luar Kota, Muaro Jambi, Jambi 36361, Indonesia*
[c]*Department of Chemistry, Faculty of Mathematics and Natural Sciences, Universitas Gadjah Mada, Bulaksumur, Depok, Sleman, Yogyakarta 55281, Indonesia*
[d]*Research Center for Radiation Detection and Nuclear Analysis Technology, National Research and Innovation Agency (BRIN), B.J. Habibie Science and Technology Area, 60, Raya Puspiptek str., Setu, South Tangerang 15314, Indonesia*
[*]*e-mail: latifah.hauli@brin.go.id*

Abstract. The modification of zeolite with activated charcoal for hydrogen adsorption was investigated. The aims of this research were to activate natural zeolite (Z), modify Z with commercial activated charcoal (AC/Z), and study the properties of these materials for hydrogen storage. The Z was prepared by the desilication method. The obtained Z was modified by activated charcoal using the wet impregnation method. The obtained materials were characterised by surface area analyser, X-ray diffraction, fourier transform infrared spectroscopy, and scanning electron microscopy with energy dispersive spectrometry. The hydrogen storage performance (at 298 K and 1 atm) was observed by Hydrogen-temperature programmed desorption (H_2-TPD). The results showed that the presence of activated charcoal on the zeolite surface increased the specific surface area, reached 188.54 m^2/g. However, Z exhibited the highest hydrogen storage capacity of 0.57 mmol/g.

Keywords: zeolite, activated charcoal, adsorbent, hydrogen storage.

Received: 30 January 2025/ Revised final: 29 April 2025/ Accepted: 2 May 2025

Introduction

Energy is a basic human need. Energy demands will increase along with the increase of population number. Currently, most of the world's energy needs are met by using fossil energy sources (petroleum, natural gas, and coal). However, the source of fossil energy is dwindling. Excessive use of fossil fuels also gives a negative impact on the environment and the health of living things. Beside producing energy, burning fossil energy sources will also produce gases, such as CO_2, NO_2 and SO_2, which can pollute the air and causes acid rain, smog, and global warming. Therefore, a renewable and environmentally friendly alternative energy source is needed to replace fossil energy [1].

Hydrogen can be an alternative energy source to replace fossil fuels. Hydrogen is an abundant element and has a higher energy content (2.75 times greater than fossil fuels) [2]. The combustion of hydrogen with oxygen will produce energy and water vapour, thus making hydrogen an environmentally friendly energy source. However, the application of hydrogen energy has several problems, especially in hydrogen storage. Several hydrogen storage technologies have been developed, such as compressed hydrogen, cryogenic-compressed liquid hydrogen tanks, metal hydrides (*e.g.*, $LaNi_5$, Mg_2Ni), chemical hydrides (*e.g.*, $LiBH_4$, $NaBH_4$ and NH_3BH_4), and adsorption on porous materials (*e.g.*, graphite nanofiber, carbon nanotubes, activated carbon, zeolite, and Metal Organic Framework). Hydrogen storage in a compressed tank or cryogenic tank has a high risk of leakage. Hydrogen storage in metal hydrides (solid storage) is safer, but the hydrogen becomes hard to release, the desorption process needs a relatively high temperature, and it may produce poisonous material. Hydrogen storage in chemical hydrides needs off-board regeneration. Hydrogen storage on porous materials is relatively safer and more

© Chemistry Journal of Moldova
CC-BY 4.0 License

efficient. Hydrogen is reversibly adsorbed on the porous material surface at a relatively high rate, resulting in rapid adsorption and desorption processes [3]. Furthermore, porous material has a low density, and the pore size can be modified. The appropriate pore size will maximize the hydrogen adsorption capacity.

Zeolite has a high potential as an adsorbent because it has a wide surface area. Natural zeolite is preferable to synthetic zeolite because of its abundance and economic value. But natural zeolite has some weaknesses, such as its non-uniform pore size, low catalytic activity, impurity, and poor crystallinity [4]. Activation and modification are needed to obtain zeolite with suitable characteristics for hydrogen absorption. The process of zeolite activation can induce the creation of mesoporous channels from the pre-existing micropore channels so that the surface area of the zeolite will increase [5]. This process will produce zeolite with 2 pore sizes, microporous (<2 nm) and mesoporous (2–50 nm), which is called hierarchical zeolite [6].

Carbon material is extensively utilised as an adsorbent in several applications [7]. Activated carbon is also a potential adsorbent for hydrogen storage. It has good chemical stability, a high surface area, and a number of narrow pores available for hydrogen adsorption, so hydrogen will get denser [3].

This work investigated Lampung natural zeolite and its modification by commercial activated charcoal for a hydrogen adsorption capacity study. Thus far, there have been no published research that have utilized Lampung natural zeolite and its composite with activated charcoal for the purpose of hydrogen storage. This study also evaluated the textural properties, crystallinity, and surface morphology of activated natural zeolite, activated charcoal, and the composite of activated charcoal-activated natural zeolite (AC/Z).

Experimental

Materials

Lampung natural zeolite was supplied from CV Minatama (Lampung, South Sumatra, Indonesia). Activated charcoal and NaOH were obtained from Merck. The NH_4NO_3 was produced by Smart-Lab Indonesia. All chemical material is of analytical grade and was used without further treatment.

Procedure for sample preparation

The natural zeolite activation (Z) was performed by the desilication method [8]. An amount of 20 g of Lampung natural zeolite was added to 500 mL of NaOH (0.1 M) and stirred for 2 hours at a temperature of 75°C. The solid was filtered using a Buchner funnel and vacuum filtering flask and then washed using distilled water until the pH became neutral. The sample was then dried using an oven all night at a temperature of 100–110°C. The obtained solid was reacted with 150 mL NH_4NO_3 1 M for 8 hours at a temperature of 75°C. The sample was filtered, washed until the pH became neutral, and dried using an oven all night at a temperature of 100–110°C. At last, the sample was calcined at a temperature of 550°C for 2 hours.

Z modification with commercial activated charcoal (AC) was conducted by wet impregnation method. Z was dissolved in 100 mL of distilled water and stirred for 3 hours. The AC was added to Z with a weight ratio of 1:5 g/g (AC:Z) and stirred for 12 hours. The sample was then filtered and dried using oven at the temperature of 100°C for 2 hours. The obtained solid was denoted as an AC/Z. Z and AC/Z capacities for hydrogen storage were evaluated.

Characterization of sample

The textural properties of Z, AC, and AC/Z were characterized using the Quantachrome Nova 4200e. The samples were measured for N_2 adsorption and desorption at 77 K. The average catalyst pore diameter was calculated using the Barrett-Joyner-Halenda (BJH) method, and the specified surface area was calculated using the multi-point Brunauer-Emmett-Teller (BET) method by determining the desorbed N_2 area. Prior to each measurement, the samples were degassed utilizing a sample degas system at temperature of 250°C for 3 hours under nitrogen condition. Crystallinity was assessed with a Bruker X-ray diffractometer employing Co-Kα radiation. Chemical interactions were analysed using a Bruker Tensor 27 FTIR Spectrophotometer, while morphology was examined with a SEM JEOL JSM-IT200 equipped with an EDX detector. The evaluation of hydrogen adsorption and desorption for the samples was conducted using the Hydrogen-temperature programmed desorption (H_2-TPD) instrument, specifically the Micromeritics Chemisorb 2750. Before measurement, the sample was heated at 200°C for 180 min under helium gas conditions. Then, the temperature was lowered to room temperature. Adsorption of H_2 was carried out at room temperature for 60 minutes, then purged with argon gas (inert) at the same temperature for 30 minutes. H_2 desorption was carried out at room temperature –500°C with a temperature increase rate of 10°C/min.

Results and discussion

Evaluation of textural properties

The textural properties analysis result (Table 1) shows that the addition of AC to Z, which has a high surface area, enhances the textural properties of Z. The commercial activated charcoal has the highest surface area of 911.30 m^2/g. The surface area of Z increases by 38% (from 136.35 m^2/g to 188.54 m^2/g), the total pore volume increases by 2% (from 0.28 cm^3/g to 0.29 cm^3/g), and the average pore diameter decreases by 25% (from 8.11 nm to 6.07 nm). However, this composite value is lower than the textural properties of a similar composite of activated carbon and zeolites. Li, H. *et al*., reported that the composite of zeolite and activated carbon had surface area of 520.4 m^2/g for coal-based zeolite-activated carbon and 879.1 m^2/g for bamboo-based zeolite-activated carbon [9]. This difference showed that the composition of activated carbon and the source of zeolite has an important role in determining the composite surface area.

The nitrogen adsorption-desorption for Z, AC, and AC/Z samples are shown in Figure 1. All samples follow isotherm type IV. The observed phenomenon is in line with capillary condensation occurring in mesopores, and the maximum amount of substance absorbed is limited within a range of high relative pressure to saturation pressure [10]. They also have hysteresis loop, indicating the formation of mesoporous and micropore structure [11], as confirmed with the textural properties analysis result in Table 1.

XRD characterization

The XRD spectra of Z indicate a good crystallinity, as shown in Figure 2. Most of the peaks have sharp diffraction that can be attributed to clinoptilolite. The similar diffraction pattern is observed for hierarchical NaX and BaX zeolites [12]. Meanwhile, AC has a broad diffraction band, which means that AC has a low structural ordering [13]. Two major peaks at 2θ around 30° and 50° are known to be a characteristic pattern of disordered graphite-like structure of amorphous carbon [1]. Based on the diffraction pattern of AC/Z, that composite has similar diffraction pattern and crystallinity to Z. It means that the addition of activated carbon does not interfere with the crystallinity properties of activated natural zeolite. It may happen because the composition of AC in the composite is low. A higher composition of activated carbon in composite with hierarchical zeolite will show a steamed bread-shape curve in the XRD patterns which demonstrates the combination of activated carbon and zeolites in the composite [9].

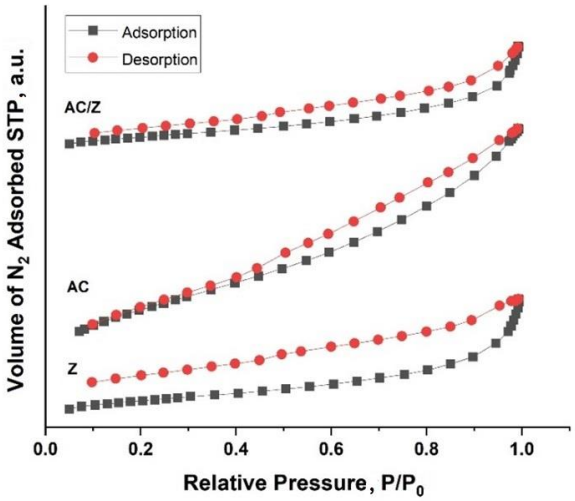


Figure 1. Isotherm of N_2 adsorption-desorption of the samples.

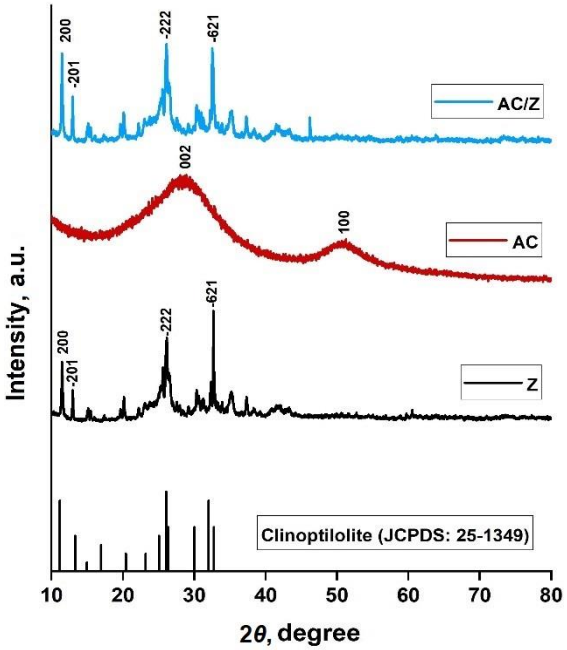


Figure 2. XRD patterns of the samples.

Table 1

Textural properties of the samples.

Sample	*Surface area (m^2/g)*	*Average pore diameter (nm)*	*Total pore volume (cm^3/g)*	*Micropore volume (cm^3/g)*	*Mesopore volume (cm^3/g)*
Z	136.35	8.11	0.276	0.036	0.240
AC	911.30	3.66	0.833	0.357	0.476
AC/Z	188.54	6.07	0.286	0.048	0.238

FTIR characterization

The FTIR spectra of Z and AC/Z samples are similar, as shown in Figure 3. The peaks appear at wavenumbers of about 480, 500, 790, 1100, 1600, and 3400 cm^{-1}. The internal framework of T–O–T, where T is both Al and Si, is shown at a band around 480 cm^{-1}. The pentasil ring vibration of zeolite topology is shown at band around 500 cm^{-1} [11]. The bands around 790 and 1100 cm^{-1} regions are assigned to the characteristic asymmetric and symmetric stretching modes of Si–O–Si, respectively. The OH bending vibration is appeared with a strong band at about 1600 cm^{-1} and a broad band at about 3400 cm^{-1}. The broad band around 3500 cm^{-1} also indicates the presence of Si–OH groups [14]. Meanwhile, the peak at 1570 cm^{-1} in AC indicates the aromatic C=C ring stretching and the broad band seen around 3400 cm^{-1} is generated by the stretching of O–H bonds [15].

SEM-EDS characterization

The surface morphology of Z and AC/Z samples is presented in Figure 4. The morphology indicates that Z and AC/Z are irregular in shape and uniform in size and are observed to form agglomerations. This observed effect is possible due to the zeolite activation process. The use of NH_4NO_3 serves as an ion-exchange agent in the zeolite activation process. Zeolite treated with desilication was then activated with NH_4NO_3. Cations such as Na^+, K^+, Mg^{2+}, and Ca^{2+} present in natural zeolite can be exchanged by NH_4^+ generated by NH_4NO_3. The cation exchange in zeolite with NH_4^+ aims to replace the cations, leading to zeolite- NH_4^+. During the calcination process, NH_4^+ may be dissociated into NH_3 gas. This changes zeolite-NH_4^+ into zeolite-H, which has a hierarchical structure with micropores and mesopores. This activation step can indeed influence the morphology and porosity of Z. The addition of NH_4NO_3 can occasionally result in more uniform sizes or change the porosity of the end product. The presence of activated charcoal is readily apparent on the surface of the AC/Z composite, while Z is also detected on the activated charcoal surface. This indicates that the AC/Z composite is successfully synthesized.

The EDS results presented in Figure 5, which depicted the carbon intensity in the AC/Z composite, further confirmed this finding. The composition of each specific element, including Si, O, Al, and C in Z and AC/Z samples, has been summarized and presented in Table 2. When activated carbon is introduced, additional carbon content is incorporated into the sample, altering the overall composition and affecting the relative Si percentage. The change does not necessarily indicate a reduction in the absolute amount of Si but rather a redistribution of elemental ratios due to the presence of AC. This condition does not only occur in Si, which experiences changes, but a decrease in content is observed in all elements in the AC except carbon.

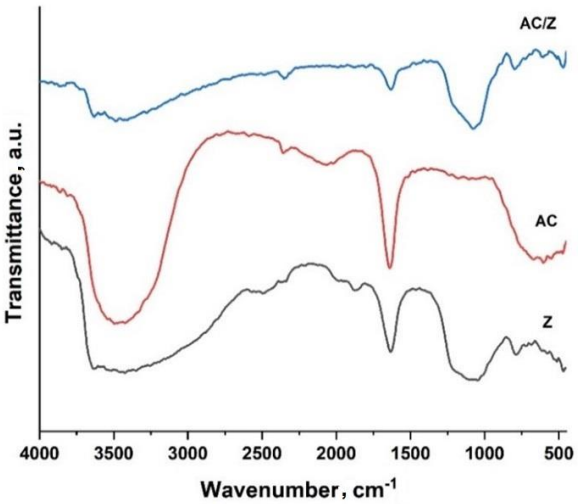
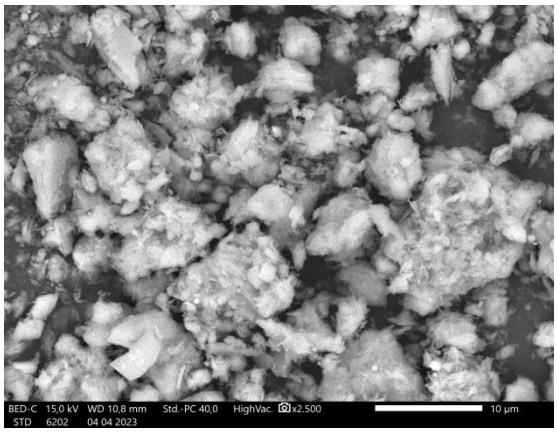
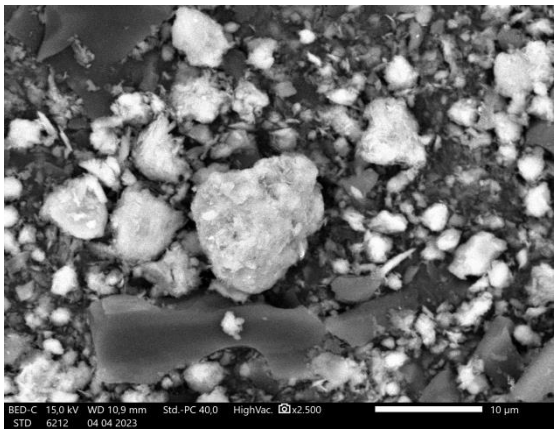


Figure 3. FTIR spectra of the samples.

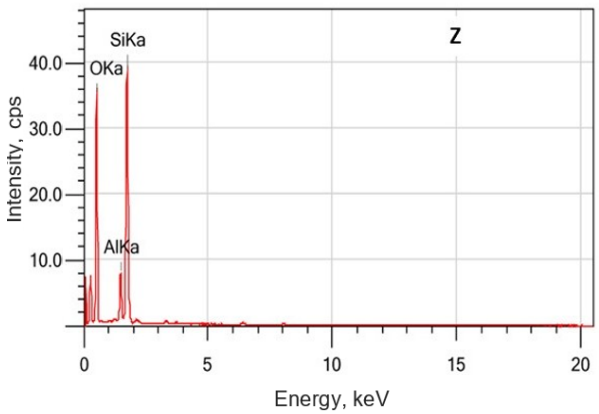


(a)

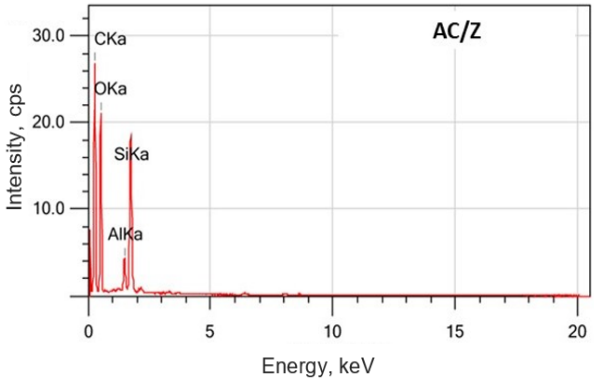


(b)

Figure 4. SEM images of Z *(a)* and AC/Z *(b)* samples.



(a)



(b)

Figure 5. EDS of Z *(a)* and AC/Z *(b)* samples.

Table 2

Element content of the samples.

Sample	*Element content (wt.%)*			
	Si	*Al*	*O*	*C*
Z	32.54	6.05	61.41	-
AC/Z	6.67	1.46	41.06	50.81

Hydrogen adsorption performance

H_2-TPD is an instrument used to study the impact of activated charcoal on H_2 adsorption behaviour when combined with zeolite. In this study, the H_2 adsorption capacity was measured at room temperature for 60 minutes with a pressure of 1 atm. Figure 6 presents the H_2-TPD profiles of the samples at room temperature and a pressure of 1 atm. It is obvious that the samples exhibit two peaks of H_2 desorption in their TPD patterns. The Z and AC/Z samples are identified as having similar patterns. Two peaks are observed at desorption temperatures around 200°C and 450°C. The AC sample, on the other hand, lacked a distinct desorption peak and revealed a very low intensity. The desorption peak seen at a temperature of 100°C is attributed to the H_2 molecules that are only weakly adsorbed onto the surface of the sample. This is seen in the AC sample, which has a significantly diminished peak intensity. The desorption peak at a temperature of 200–450°C corresponds to strongly adsorbed H_2 on the sample. Samples Z and AC/Z demonstrate this condition. Despite its apparent similarity in pattern, the strength of H_2 adsorption on AC/Z is found to be lower compared with that of Z. This phenomenon is discovered because the initial peak of hydrogen desorption on AC/Z occurs at a temperature below 200°C. The first peak corresponds to weakly adsorbed hydrogen, which is likely physisorbed within or on the surface of the samples. The second peak represents more strongly adsorbed hydrogen, possibly due to interactions with specific active sites in the zeolite framework.

The values for the H_2 adsorption capacities of the samples are summarized in Table 3. AC/Z has a lower adsorption capacity value than Z, namely 0.47 mmol/g. In addition, Z was observed to have the highest adsorption capacity, namely 0.57 mmol/g. The measured AC has the lowest hydrogen adsorption capacity, namely 0.06 mmol/g. Under standard conditions of room temperature and 1 atmosphere pressure, it has been demonstrated that AC does not have a substantial effect on the maximum adsorption of hydrogen, despite its highly large surface area. Meanwhile, Z can absorb hydrogen more effectively under same conditions. This phenomenon might arise as a result of the interaction between the active functional groups present in the zeolite and H_2 [16].

Table 3

H_2 adsorption capacity of the sample.

Sample	*H_2 Adsorption capacity (mmol/g)*
Z	0.57
AC	0.06
AC/Z	0.47

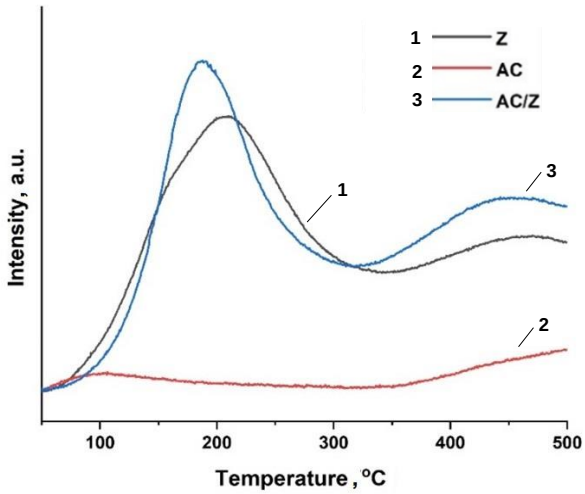


Figure 6. Hydrogen-temperature programmed desorption (H_2-TPD) of the samples.

This condition also occurs in AC/Z. AC does not have active groups on its surface, but the presence of zeolite in AC/Z allows it to adsorb H_2 at room temperature and 1 atm pressure. AC, which does not have surface active groups, is capable of maximum hydrogen adsorption at lower temperatures or under higher pressure conditions, as reported by Mohan, M. *et al.* [17] and Zieliński, M. *et al.* [18]. Despite its large surface area, the pore structure of AC is not consistently favourable to effective hydrogen storage, especially at room temperature. The size and interconnectivity of the pores may inhibit hydrogen molecules from infiltrating the material thoroughly, hence diminishing the effective surface area accessible for adsorption.

The adsorption mechanism of hydrogen (H_2) on zeolite (Z) is influenced by parameters like surface area, porosity, and active functional groups. Since H_2 is a nonpolar molecule, its interaction with zeolite mostly occurs through physisorption (Van der Waals forces) in zeolites with a large surface area and microporosity, which offer numerous adsorption sites. Zeolites require modifications like metal doping (Ni, Pd, Pt, *etc*.) or functionalization with active groups to enhance their adsorption capacity of H_2 by chemisorption. The existence of other metals in zeolite, including balancing metal cations that may not be completely removed during the activation process, as well as the presence of aluminium in the zeolite framework, would also likely influence the enhancement of hydrogen adsorption capacity. The interaction of active metals in zeolites and H_2 molecules can occur chemically through a spillover process. In the spillover process, hydrogen atoms migrated to the zeolite surface as hydrogen molecules attached to the metal surface without forming bonds between them. The bonds between hydrogen atoms (H–H) become unstable because of the spillover effect, facilitating the dissociation of H–H bonds and the release of H atoms. A higher number of H atoms are going to enter into the support pore compared to H_2 molecules, resulting in increased adsorption [19]. However, in the current study, metal impregnation was not conducted. This interaction possible could occur within the aluminium metal of the zeolite framework. The process of desilication on Z also has an impact on the presence of aluminium. It reduces the Si content and decreases the Si/Al ratio, which means more aluminium in the structure. It can potentially influence the interaction between H_2 and Al, leading to an increase in hydrogen adsorption. This study indicates that Z has a higher capacity to adsorb hydrogen compared to AC or AC/Z under conditions of room temperature and 1 atmosphere pressure.

Conclusions

The hydrogen storage performance of Z, AC, and AC/Z samples has been investigated. Z was activated using the desilication method, and AC/Z was synthesized using the wet impregnation method. The obtained materials in this work were characterized by SAA, XRD, FTIR, SEM-EDS, and H_2-TPD. The AC/Z composite sample exhibited a higher surface area than Z, measuring 188.54 m^2/g. XRD characterization also demonstrated the similar diffraction pattern and crystallinity between Z and AC/Z. The crystalline structure of Z was predominantly composed of the clinoptilolite phase. The morphology of Z and AC/Z indicated the irregular in shape and uniform in size and tend to form agglomerations. The success of zeolite modification with activated carbon was revealed by the EDS results, which showed the presence of carbon composition. However, the hydrogen storage investigation under conditions of room temperature and 1 atmosphere pressure revealed that Z was capable of hydrogen adsorption, with a capacity value of 0.57 mmol/g.

Acknowledgments

The authors acknowledge the facilities and scientific and technical support from Advanced Characterization Laboratories Serpong, the National Research and Innovation Agency (BRIN) through E-Layanan Sains.

References

1. Ramesh, T.; Rajalakshmi, N.; Dhathathreyan, K.S. Synthesis and characterization of activated carbon from jute fibers for hydrogen storage. Renewable Energy and Environmental Sustainability, 2017, 2(4), pp. 1–8. DOI: https://doi.org/10.1051/rees/2017001
2. Sethia, G.; Sayari, A. Activated carbon with optimum pore size distribution for hydrogen storage. Carbon, 2016, 99, pp. 289–294. DOI: https://doi.org/10.1016/j.carbon.2015.12.032
3. Md Arshad, S.H.; Ngadi, N.; Aziz, A.A.; Amin, N.S.; Jusoh, M.; Wong, S. Preparation of activated carbon from empty fruit bunch for hydrogen storage. Journal of Energy Storage, 2016, 8, pp. 257–261. DOI: https://doi.org/10.1016/j.est.2016.10.001
4. Neolaka, Y.A.B.; Supriyanto, G.; Kusuma, H.S. Synthesis and characterization of natural zeolite with ordered ion imprinted polymer structures (IIP@AFINZ) for selective Cr(VI) adsorption from aqueous solution. Moroccan Journal of Chemistry, 2019, 7(1), pp. 194–210. DOI: https://doi.org/10.48317/IMIST.PRSM/morjchem-v7i1.14879

5. Kerstens, D.; Smeyers, B.; Van Waeyenberg, J.; Zhang, Q.; Yu, J.; Sels, B.F. State of the art and perspectives of hierarchical zeolites: practical overview of synthesis methods and use in catalysis. Advanced Materials, 2020, 32(44), pp. 1–52. DOI: https://doi.org/10.1002/adma.202004690
6. Li, K.; Valla, J.; Garcia-Martinez, J. Realizing the commercial potential of hierarchical zeolites: New opportunities in catalytic cracking. ChemCatChem, 2014, 6(1), pp. 46–66. DOI: https://doi.org/10.1002/cctc.201300345
7. Mahardiani, L.; Saputro, S.; Mahmud Zinki, N.M. One pot synthesis of carboxylated activated carbon for water purification: A kinetic study. Moroccan Journal of Chemistry, 2020, 8(4), pp. 957–964. DOI: https://doi.org/10.48317/IMIST.PRSM/morjchem-v8i4.21727
8. Kurniawati, D.; Jumaeri, J.; Tursiloadi, S.; Arutanti, O.; Safaat, M. Modification of Indonesian natural zeolite (clipnotillite-mordenite) for synthesis of solketal. Iranian Journal of Catalysis, 2021, 11(3), pp. 295–302. DOI: https://oiccpress.com/ijc/article/view/3604
9. Li, H.; Li, M.; Zheng, F.; Wang, J.; Chen, L.; Hu, P.; Zhen, Q.; Bashir, S.; Liu, J.L. Efficient removal of water pollutants by hierarchical porous zeolite-activated carbon prepared from coal gangue and bamboo. Journal of Cleaner Production, 2021, 325, p. 129322. DOI: https://doi.org/10.1016/j.jclepro.2021.129322
10. Sing, K.S.W. Reporting physisorption data for gas/solid systems with special reference to the determination of surface area and porosity (Recommendations 1984). Pure and Applied Chemistry, 1985, 57(4), pp. 603–619. DOI: https://doi.org/10.1351/pac198557040603
11. Iryani, A.; Masudi, A.; Rozafia, A.I.; Hartanto, D.; Santoso, M.; Nur, H.; Azami, M.S. Enhanced removal of soluble and insoluble dyes over hierarchical zeolites: Effect of synthesis condition. Inorganics, 2020, 8(9), pp. 52–70. DOI: https://doi.org/10.3390/INORGANICS8090052
12. Medeiros-Costa, I.C.; Laroche, C.; Pérez-Pellitero, J.; Coasne, B. Characterization of hierarchical zeolites: Combining adsorption/intrusion, electron microscopy, diffraction and spectroscopic techniques. Microporous and Mesoporous Materials, 2019, 287, pp. 167–176. DOI: https://doi.org/10.1016/j.micromeso.2019.05.057
13. Zhao, W.; Fierro, V.; Zlotea, C.; Izquierdo, M.T.; Chevalier-César, C.; Latroche, M.; Celzard, A. Activated carbons doped with Pd nanoparticles for hydrogen storage. International Journal of Hydrogen Energy, 2012, 37(6), pp. 5072–5080. DOI: https://doi.org/10.1016/j.ijhydene.2011.12.058
14. Ghanbari, B.; Kazemi Zangeneh, F.; Taheri Rizi, Z.; Aghaei, E. High-impact promotional effect of Mo impregnation on aluminum-rich and alkali-treated hierarchical zeolite catalysts on methanol aromatization. ACS Omega, 2020, 5(21), pp. 11971–11986. DOI: https://doi.org/10.1021/acsomega.9b04407
15. Zhao, Y.; Cho, C.-W.; Cui, L.; Wei, W.; Cai, J.; Wu, G.; Yun, Y.-S. Adsorptive removal of endocrine-disrupting compounds and a pharmaceutical using activated charcoal from aqueous solution: kinetics, equilibrium, and mechanism studies. Environmental Science and Pollution Research, 2019, 26, pp. 33897–33905. DOI: https://doi.org/10.1007/s11356-018-2617-7
16. Tursiloadi, S.; Wahyuni, A.; Marlinda, L.; Safaat, M.; Hauli, L.; Manulang, W.F.; Amin, A.K.; Khaerudini, D.S.; Al Muttaqii, M. Modification of natural zeolite from Bogor for hydrogen storage. Rasayan Journal of Chemistry, 2023, 16(4), pp. 2345–2352. DOI: https://doi.org/10.31788/RJC.2023.1648306
17. Mohan, M.; Sharma, V.K.; Kumar E.A.; Gayathri, V. Hydrogen storage in carbon materials - A review. Energy Storage, 2019, 1(2), e35, pp. 1–26. DOI: https://doi.org/10.1002/est2.35
18. Zieliński, M.; Wojcieszak, R.; Monteverdi, S.; Mercy, M.; Bettahar, M.M. Hydrogen storage in nickel catalysts supported on activated carbon. International Journal of Hydrogen Energy, 2007, 32(8), pp. 1024–1032. DOI: https://doi.org/10.1016/j.ijhydene.2006.07.004
19. Nishihara, H.; Hou, P.-X.; Li, L.-X.; Ito, M.; Uchiyama, M.; Kaburagi, T.; Ikura, A.; Katamura, J.; Kawarada, T.; Mizuuchi, K.; Kyotani, T. High-pressure hydrogen storage in zeolite-templated carbon. The Journal of Physical Chemistry C, 2009, 113(8), pp. 3189–3196. DOI: https://doi.org/10.1021/jp808890x